

Title no. 110-S11

Shake-Table Studies of Repaired Reinforced Concrete Bridge Columns Using Carbon Fiber-Reinforced Polymer Fabrics

by Ashkan Vosooghi and M. Saiid Saiidi

The main objective of this study was to develop a rapid and effective repair method using carbon fiber-reinforced polymer (CFRP) fabrics for earthquake-damaged reinforced concrete (RC) bridge columns. Shake-table studies, repair methods, and test results are discussed in this paper. One standard bent of a two-span bridge model with two low-shear columns, two standard high-shear columns, and one low-shear and one high-shear substandard column were tested on shake tables. The column models were repaired using CFRP fabrics; fast-setting, nonshrink repair mortar; and epoxy injection and retested on shake tables to evaluate the performance of the repair procedure. The results indicated that the strength and displacement capacity of the standard columns were successfully restored and those of the substandard columns were upgraded to meet current seismic standards after the repair. However, the stiffness was not restored due to material degradation during the original tests.

Keywords: carbon fiber-reinforced polymer fabric; earthquake damage; emergency repair; reinforced concrete bridge column; repair; shake-table test.

INTRODUCTION

The current earthquake engineering design practice for ordinary bridges allows for damage to bridge columns during moderate and strong earthquakes. The target response under the maximum considered earthquake is “no-collapse,” realizing that the structure would undergo considerable nonlinearity associated with extensive concrete damage, yielding of bars, or even rupture of a limited number of the bars. For the more frequent earthquakes, the target response is repairable damage that would allow for relatively rapid restoration of the bridge. The level of damage to different columns of a bridge varies depending on the intensity of the ground shaking, type of earthquake, and the force and deformation demand on individual members. Based on the inspection of the damaged columns, engineers have to determine whether the bridge is sufficiently safe to be kept open to traffic without repair, whether it is repairable within a reasonable time frame, or if it needs to be replaced. This study was aimed at developing a reliable and efficient repair procedure for earthquake-damaged reinforced concrete (RC) bridge columns using carbon fiber-reinforced polymers (CFRPs).

Although there are numerous studies on seismic *retrofit* of RC columns (Saadatmanesh et al. 1996; Seible et al. 1997; Haroun and Elsanadedy 2005; Laplace et al. 2005), only a few studies have focused on seismic *repair* (Priestley and Seible 1993; Saadatmanesh et al. 1997; Lehman et al. 2001; Li and Sung 2003; Saiidi and Cheng 2004; Belarbi et al. 2008). In these studies, the damaged concrete was replaced with new concrete and the cracks were epoxy-injected. The buckled or fractured bars were replaced with new bars (Lehman et al. 2001) or replaced with equivalent fiber-reinforced polymer (FRP) fabrics (Saiidi and Cheng 2004; Belarbi et al. 2008). The repaired columns were serviceable after full curing of

new concrete in at least 28 days. In addition, replacing fractured bars was complicated and time-consuming because it required removing a significant amount of concrete from the damaged zone and adjacent footing. The techniques could not be considered “rapid repair.” In this study, fast-setting repair mortar and accelerated CFRP jacket curing were used to restore service in less than 1 week. This type of repair may be labeled as “emergency” repair due to its urgency and the speed of repair work.

Shake-table studies of repaired bridge column models are presented in this paper. Original column models were tested on a shake table until reaching the highest target repairable damage state. They were subsequently repaired using unidirectional CFRP fabrics with fibers in the hoop direction and retested on the shake table until failure to evaluate the repair performance.

RESEARCH SIGNIFICANCE

Delay in opening an earthquake-damaged bridge to traffic can have severe consequences on the passage of emergency response vehicles, detour lengths, and traffic congestion. Rapid and effective repair methods are needed to enable quick opening of the bridge to minimize impact on the community and beyond. In this study, a rapid repair procedure using CFRP fabrics was developed and evaluated for RC bridge columns. The experimental studies indicated that a damaged column can be repaired in only a few days using CFRP fabrics. The proposed repair method using CFRP fabrics can be very useful in emergency repair of earthquake-damaged bridges.

DESCRIPTION OF TEST MODELS

One standard bent consisting of two low-shear columns (Bent-2), two standard high-shear columns (NHS1 and NHS2), one low-shear substandard column (OLS), and one high-shear substandard column (OHS) were studied. Columns meeting current seismic design requirements are referred to as “standard” columns. Other columns are labeled as “substandard.”

Two-column bent

Choi et al. (2007) tested a one-fourth-scale, two-span bridge model supported on three two-column piers using three shake tables at the University of Nevada, Reno (Fig. 1(a)). The seismic design of the bridge was based on recent seismic design guidelines (Johnson et al. 2008). The

ACI Structural Journal, V. 110, No. 1, January-February 2013.

MS No. S-2011-066.R4 received November 18, 2011, and reviewed under Institute publication policies. Copyright © 2013, American Concrete Institute. All rights reserved, including the making of copies unless permission is obtained from the copyright proprietors. Pertinent discussion including author's closure, if any, will be published in the November-December 2013 *ACI Structural Journal* if the discussion is received by July 1, 2013.

ACI member **Ashkan Vosooghi** is a Postdoctoral Fellow in the Department of Civil and Environmental Engineering at the University of Nevada, Reno, NV (UNR). He received his BSC from Isfahan University of Technology, Isfahan, Iran; his MSCE in earthquake engineering from the International Institute of Earthquake Engineering and Seismology, Tehran, Iran; and his PhD in structural/earthquake engineering from UNR with an emphasis on bridge engineering in 1999, 2002, and 2010, respectively. His research interests include seismic design, retrofit, and repair of structures.

M. Saïid Saïidi, F.A.C.I., is a Professor of Civil & Environmental Engineering and the Director of the Center for Advanced Technology in Bridges and Infrastructure at UNR. He is the founding and former Chair and a current member of ACI Committee 341, Earthquake-Resistant Concrete Bridges. He is also a member of Joint ACI-ASCE Committee 352, Joints and Connections in Monolithic Concrete Structures, and ACI Subcommittee 318-D, Flexure and Axial Loads: Beams, Slabs, and Columns.

measured yield stress of the longitudinal bars and spirals was 67.9 and 55.8 ksi (468 and 385 MPa), respectively, and the measured concrete compressive strength was 6.47 ksi (44.6 MPa) on the test day. Because the middle bent was the most severely damaged pier, it was used in the emergency repair study. The original middle bent was designated as Bent-2 and the repaired bent was designated as Bent-2R. Bent-2 was composed of two columns that spanned a distance of 75 in. (1.9 m) center to center. The details of the column sections are shown in Fig. 1(d).

The axial load index is defined as the compressive axial force due to gravity loads divided by the product of the cross-section area of the column and the specified concrete compressive strength. Based on Caltrans design practice, this index typically varies from 5 to 10% in bridge columns,

and it was 8.2% in the two-span bridge model (Johnson et al. 2008). The average shear stress is calculated as the ratio of the plastic shear divided by the effective shear area. The effective shear area is taken as 80% of the gross section area A_g in circular columns (Caltrans 2006). The shear stress index is calculated by dividing the average shear stress by $\sqrt{f'_c}$ (psi) ($0.083\sqrt{f'_c}$ [MPa]). This index is used to determine the level of shear stress in columns. In this study, an index smaller than 4 was treated as the low shear level in the column. The columns in Bent-2 were flexure-dominated with a shear index of 2.3.

Columns NHS1 and NHS2

As part of this study, two similar standard high-shear RC bridge columns were studied (Vosooghi and Saïidi 2010a). NHS1 and NHS2 (new design high shear) are the designations of the two original column models (Fig. 1(b) and (d)). The repaired models were labeled NHS1-R and NHS2-R. The designation of “new” indicates that the column meets current seismic code requirements. The models were flexure-dominated, as the current codes do not allow shear-dominated columns. However, the level of shear was relatively high in NHS1 and NHS2 with the shear index being 6.12. NHS1 and NHS2 were constructed at different times because the study of NHS2 was found to be necessary after NHS1-R testing and analysis of the data. The latest Caltrans Seismic Design Criteria (SDC) (version 1.4) (Caltrans 2006) and Bridge Design Specifications (Caltrans 2003) were used to

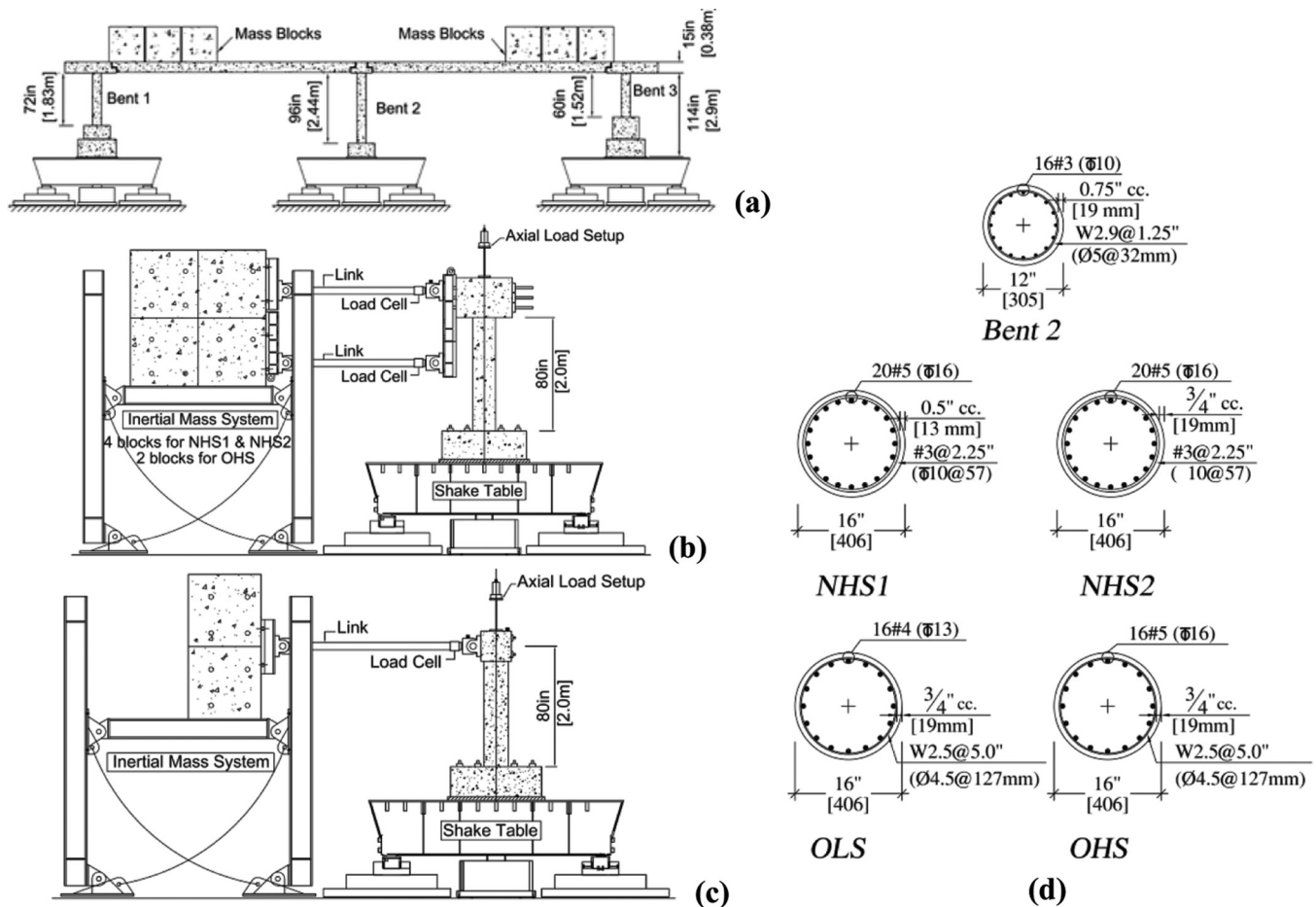


Fig. 1—Shake-table setup and column model details: (a) two-span bridge; (b) double-curvature column; (c) cantilever column; and (d) column sections.

design the columns. The axial load index was 10% for the column models. The measured yield stresses of the longitudinal bars and spirals of NHS1 were 73.5 and 60.6 ksi (507 and 418 MPa), and those of NHS2 were 66.5 and 67.0 ksi (458 and 462 MPa), respectively. The measured concrete compressive strengths in NHS1 and NHS2 were 7.29 and 6.17 ksi (50.3 and 42.5 MPa), respectively, on the test day.

Columns OLS and OHS

RC bridge columns designed prior to the 1970s were not adequately detailed to resist seismic loads and are considered to be substandard. They have insufficient lateral reinforcement and their longitudinal bars are lap-spliced at the base.

As part of this study, one substandard low-shear and one substandard high-shear RC bridge column were studied (Vosooghi and Saiidi 2010a). OLS and OHS are the designations used for the old design low shear and the old design high shear column models, respectively, and OLS-R and OHS-R are the designations used for the repaired columns. The designation of “old” indicates that the columns do not meet current seismic code requirements. The details of the columns are shown in Fig. 1(b) through (d). The axial load index was 7.5% for both columns and the shear indexes were 1.9 and 5.2 for OLS and OHS, respectively.

Prior to the 1970s, Grade 40 and 50 steel was used in RC construction. Due to the unavailability of Grade 40 bars, Grade 60 steel was used in the column models and the steel ratio was modified proportionally. The measured yield stresses of the longitudinal bars in OLS and OHS were 64.5 and 66.5 ksi (445 and 458 MPa), respectively. The measured yield stress of hoops was 60.0 ksi (414 MPa) in both columns. The measured concrete compressive strengths in OLS and OHS were 4.94 and 4.97 ksi (34.0 and 34.3 MPa), respectively, on the test day. The lap-splice length varies from 20 to 30 times the longitudinal bar diameter d_b in substandard columns. The splice length of $24d_b$ was selected (Laplace et al. 2005). Because the required length of the splice is proportional to steel yield stress, it was scaled up by the factor of 3/2, which is the ratio of the specified yield stresses of Grade 60 and Grade 40 steel.

SHAKE-TABLE TEST SETUP AND TEST PROCEDURE

Different setups were used for the two-span bridge tests and single-column tests. The two-span bridge was supported on three shake tables. The superstructure consisted of six girders and was post-tensioned laterally and longitudinally to form a rigid slab. To produce the target axial load in the columns, concrete blocks and lead pallets were placed on the bridge deck (Fig. 1(a)). The original bridge model was subjected to fault-parallel near-field motions with amplitudes increasing gradually to simulate fault rupture (Choi et al. 2007).

The single-column models (NHS1, NHS2, OLS, and OHS) were tested on one of the shake tables at the University of Nevada, Reno. The inertia mass system designed by Laplace et al. (1999) was used to apply the lateral inertial force to the columns (Fig. 1(b) and (c)). A single swiveled link system or a double-link system was used to transmit the lateral inertial load from the mass rig, depending on the column. These configurations allow the columns to be tested in single or double curvature. The high shear columns were tested under double curvature (Fig. 1(b)) and the low shear column was tested under single-curvature loading (Fig. 1(c)). The footing and head of the columns were designed so they remained elastic during the shake-table tests.

The 1994 Northridge Sylmar Hospital ground motion record with peak ground acceleration (PGA) of 0.61g was selected for earthquake simulation of the single columns. This motion induced high ductility demands and residual drifts in the columns that made the repair challenging. In each shake-table test, the column was subjected to multiple simulated earthquakes—each referred to as a “run”—with gradually increasing amplitudes. In the shake-table tests of the original bent and columns, the amplitude of each run was determined such that no steel bars fractured during the tests. The number of runs was kept as low as possible to reduce low-cycle-fatigue rupture of the longitudinal bars. The maximum strains in critical bars in the plastic hinge zone were carefully monitored for each shake-table run before deciding the amplitude of the subsequent run. In the shake-table test of the repaired bent and columns, the input motion and the loading protocols were similar to those used in the original column tests, but additional runs with higher acceleration amplitudes were applied until failure. All the models were extensively instrumented to measure strains, curvatures, displacements, forces, and accelerations.

EXPERIMENTAL RESULTS FOR ORIGINAL COLUMNS

In a previous study (Vosooghi and Saiidi 2010b), five repairable apparent damage states were identified for RC columns subjected to earthquakes. The damage states excluded failure due to bar fracture because it was believed that repair of columns with fractured bars could not be done rapidly. The damage states were defined as DS-1: flexural cracks; DS-2: minimal spalling and possible shear cracks; DS-3: extensive cracks and spalling; DS-4: visible lateral and/or longitudinal reinforcing bars; and DS-5: compressive failure of the concrete core edge (imminent failure). The five damage states are applicable to columns meeting current design codes. Substandard columns do not necessarily reach higher damage states because they are brittle.

The models were tested to reach the highest repairable damage state. The standard columns reached DS-5. At this damage state, many spirals and longitudinal bars are visible, some of the longitudinal bars begin to buckle, and the edge of the concrete core is damaged (Fig. 2). Due to severely inadequate transverse steel and longitudinal bar lap splice, the substandard columns did not undergo significant plastic deformations. Testing of Columns OLS and OHS was stopped at DS-3 and DS-2, respectively (Fig. 2), to avoid complete failure of the columns. Shear cracks covering a large area of OLS and OHS were formed during the last run. Considering the very low amount of transverse steel in these columns, it was felt that additional motions would lead to total failure of the columns, thus preventing repair.

The cumulative measured force-displacement hysteresis curves of Bent-2, NHS2, and OHS are shown in Fig. 3(a) to (c), respectively. Other test models had comparable hysteresis curves, although energy dissipation (area enclosed by the hysteresis hoops) in Column OLS was larger than that of OHS. The envelope of each hysteresis curve was determined and idealized by an elasto-plastic curve (Vosooghi and Saiidi 2010a). Using idealized force-displacement curves, the yield drift ratio, maximum drift ratio, displacement ductility, and strength of the columns were determined and are listed in Table 1. Note that the ductilities in the table are not the ductility capacities because the original columns were not tested to failure. Generally, the low shear columns (Bent-2 and OLS)

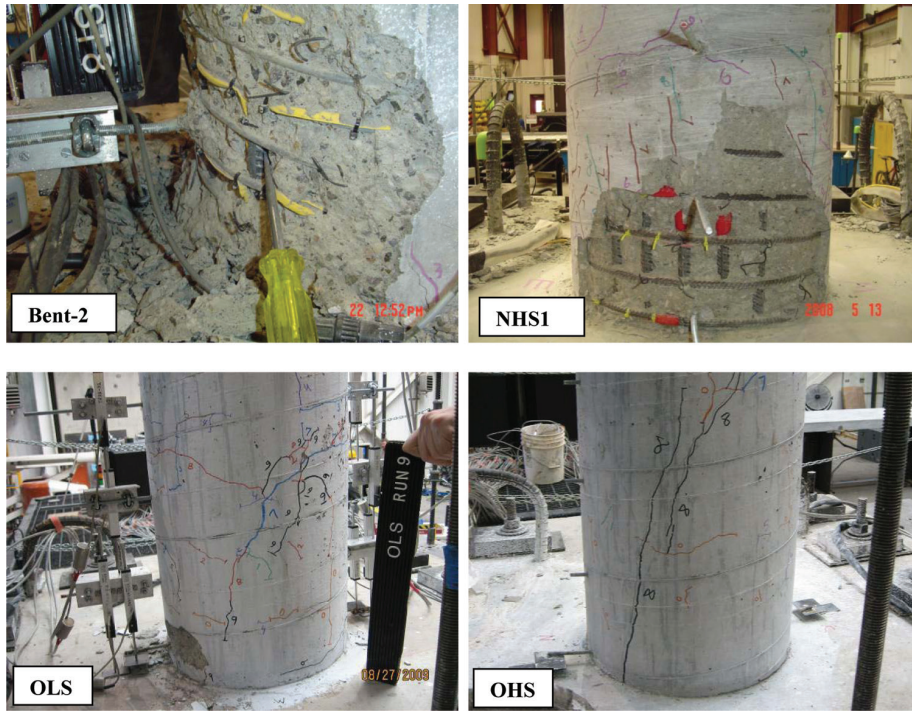


Fig. 2—Apparent damage after original shake-table tests.

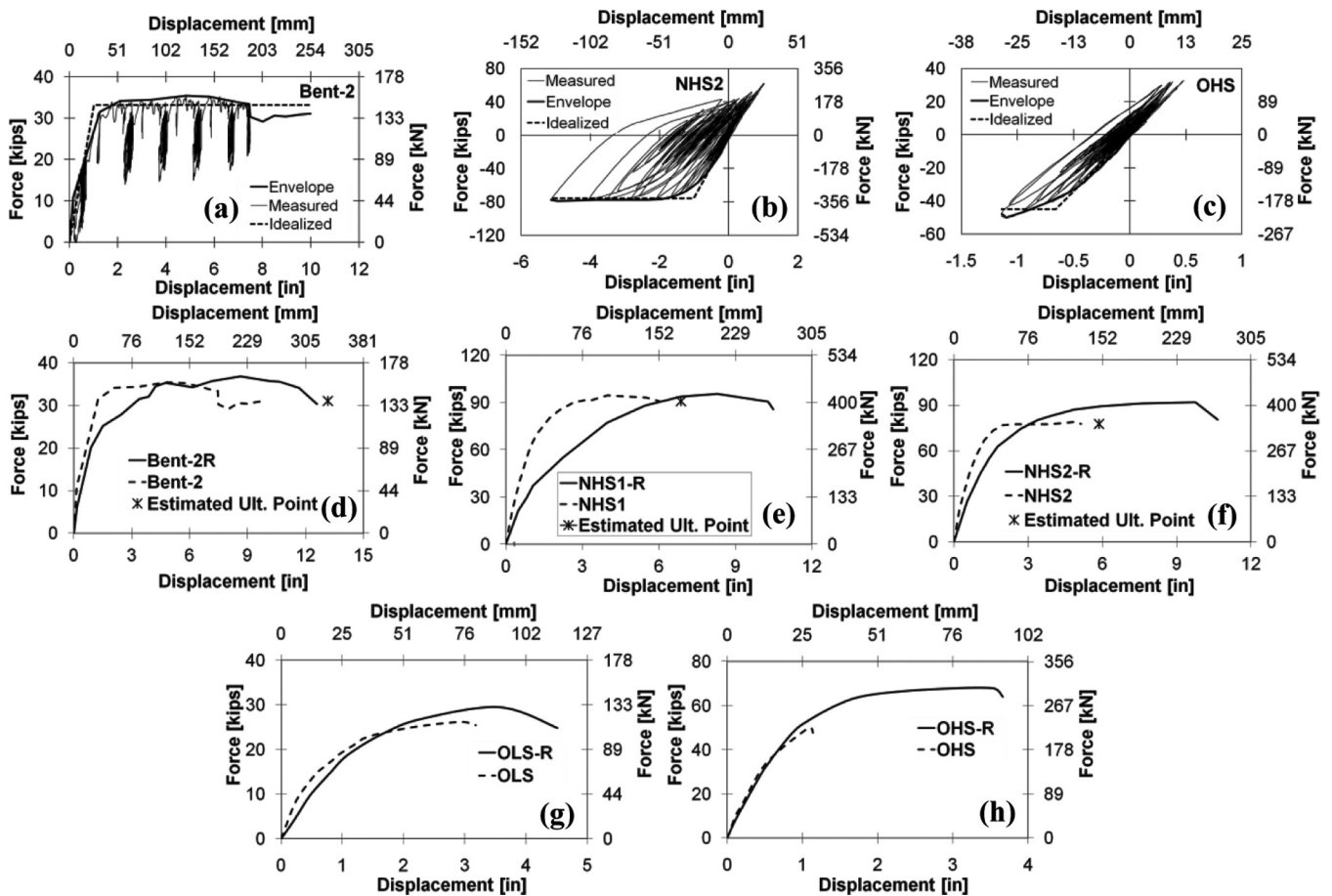


Fig. 3—Force-displacement relationships.

Table 1—Measured responses of original columns

Model	Yield drift, %	Maximum drift, %	Displacement ductility	Strength, kips (kN)	Peak strain, $\mu\epsilon$	
					Longitudinal steel	Transverse steel
Bent-2	1.06	10.41	9.8	33.2 (148)	69,868 (30 ϵ_y)	1227 (0.31 ϵ_y)
NHS1	1.58	7.54	4.8	90.5 (402)	77,522 (17.2 ϵ_y)	6510 (1.6 ϵ_y)
NHS2	1.26	6.42	5.1	75.7 (337)	54,283 (23.6 ϵ_y)	3108 (1.35 ϵ_y)
OLS	1.14	3.97	3.5	23.9 (106)	33,096 (15 ϵ_y)	6292 (1.57 ϵ_y)
OHS	0.82	1.43	1.7	45.0 (200)	23,552 (10 ϵ_y)	1340 (0.3 ϵ_y)

Note: ϵ_y is yield strain.

reached approximately two times the displacement ductility of the high shear columns at the highest repairable damage states. Because high shear induced relatively large strains in concrete, the high-shear columns reached the target damage level under smaller lateral displacements than the low-shear columns. According to Table 1, the substandard columns (OLS and OHS) reached approximately one-third of the displacement ductility of the standard columns (Bent-2 and NHS1 or NHS2) with the same level of shear because the substandard columns had severely insufficient transverse steel. For instance, OHS reached a displacement ductility of 1.7 but NHS1 and NHS2 reached a displacement ductility of 4.8 and 5.1, respectively.

The peak measured strains in the longitudinal and transverse steel of the plastic hinge zone of the columns are also listed in Table 1. The measured strains indicate that spirals in standard high-shear columns yielded during the shake-table tests; however, the spirals in standard low-shear columns remained elastic. High shears resulted in extensive shear cracks that induced large strains in the transverse steel. In substandard columns, the strains were measured in the spliced bars. In the case of splice degradation, the measured strains remain constant or decrease with increasing column lateral displacement. This was not observed; therefore, it was concluded that no slippage occurred during the shake-table tests, even though the lap-splice length was too short to develop the yield stress by 51% (ACI Committee 318 2008).

CFRP JACKET DESIGN FOR STANDARD COLUMNS

The repair of the standard column models was designed with the objective of restoring the lateral load strength and displacement capacity of the column. Unidirectional CFRP fabrics were used for this purpose. The study of other types of jackets was not within the scope of this study. The CFRP fabrics had a nominal thickness of 0.04 in. (1 mm) per layer and the fibers were in the hoop direction of the columns in all repaired models.

The CFRP jacket was designed so the repaired column could reach the plastic flexural capacity. The radial dilating strain of the jacket was limited to 4000 $\mu\epsilon$ (1 $\mu\epsilon$ = 10^{-6} in./in.) to avoid degradation in concrete aggregate interlock (Priestley et al. 1996). The contribution of concrete and spirals to shear strength was treated differently among the test models as data became available in the course of the study. Bent-2 was the first model that was tested, repaired, and retested. Due to lack of information about the contribution of concrete and spirals to the shear strength in repaired columns, their contributions were neglected conservatively along the entire column height. In the plastic hinge region, because some of the thin cracks in the core were not repairable, the shear strength of concrete was neglected in NHS1-R and NHS2-R. The spirals in NHS1 experienced a maximum

strain of approximately 1.6 times the yield strain. As a result, the shear strength of the spirals was assumed to be zero in NHS1-R. Subsequent to testing, the strain data indicated that the spirals and CFRP jacket in NHS1-R contributed to the shear strength equally. A second similar column (NHS2-R) was designed, neglecting the concrete shear strength in the plastic hinge, but the jacket was designed for one-half of the column shear demand, and the other half was assumed to be resisted by the spirals. Outside the plastic hinge region, because the spirals did not yield, the entire shear strength of the spirals was used in NHS1-R and NHS2-R. Although some shear cracks occurred outside the plastic hinge, the level of damage was much lower than that of the plastic hinges. As a result, 50% of the concrete shear strength was assumed to exist outside the plastic hinges.

Because there were no seismic *repair* design guidelines, the Caltrans (2007) seismic *retrofit* guidelines were used to restore confinement and the ductility capacity of the columns using a CFRP jacket. This document requires a confinement pressure of 300 psi (2.07 MPa) at a radial dilating strain of 4000 $\mu\epsilon$ in the plastic hinge regions. The confinement pressure can be reduced to 150 psi (1.03 MPa) at the same dilating strain outside the plastic hinges.

The required and actual thicknesses of the CFRP jackets are listed in Table 2. In Bent-2R, the jacket consisted of two layers of CFRP at the plastic hinge regions and one layer of CFRP elsewhere. The Caltrans (2007) confinement requirements governed the jacket design in the plastic hinge regions and shear strength governed the jacket design outside the plastic hinge regions. In Bent-2R, the end 18 in. (457 mm) (one-and-a-half-column diameter) was assumed to be the primary plastic hinge zone and the adjacent 12 in. (304.8 mm) (one-column diameter) was treated as the secondary plastic hinge zone. There was a concern that plastic deformation could extend beyond the primary plastic hinge zone; hence, the number of CFRP layers in the primary plastic hinge was maintained in the secondary plastic hinge (Seible et al. 1997).

In NHS1-R, the jacket consisted of four layers of CFRP at the plastic hinge regions and one layer of CFRP elsewhere. The shear strength governed the jacket design in the plastic hinge regions and the Caltrans (2007) confinement requirements controlled the jacket design outside the plastic hinge regions. In NHS2-R, the jacket consisted of two layers of CFRP at the plastic hinge regions and one layer of CFRP elsewhere. Table 2 shows that the Caltrans (2007) confinement requirements governed the jacket design inside and outside the plastic hinge regions of NHS2-R. In NHS1-R and NHS2-R, a length of 24 in. (610 mm) was used for the plastic hinge regions (one-and-a-half-column diameter). The test results for Bent-2R indicated that plastic hinging did not extend into the secondary plastic hinge regions. Consequently, no secondary plastic hinge region was considered in

Table 2—Thickness of CFRP jackets in repaired columns

Test model	Location	Shear strength, in. (mm)	Lap splice, in. (mm)	Confinement, in. (mm)	Actual, in. (mm)
Bent-2R	OPHR	0.0345 (0.88)	NA (NA)	0.0281 (0.71)	0.04 (1.0)
	IPHR	0.0345 (0.88)	NA (NA)	0.0563 (1.43)	0.08 (2.0)
NHS1-R	OPHR	0.024 (0.61)	NA (NA)	0.038 (0.97)	0.04 (1.0)
	IPHR	0.138 (3.51)	NA (NA)	0.075 (1.91)	0.16 (4.0)
NHS2-R	OPHR	0.002 (0.05)	NA (NA)	0.03 (0.76)	0.04 (1.0)
	IPHR	0.049 (1.24)	NA (NA)	0.06 (1.52)	0.08 (2.0)
OLS-R	OPHR	0.008 (0.20)	0 (0)	0.025 (0.64)	0.04 (1.0)
	IPHR	0.022 (0.56)	0.080 (2.0)	0.05 (1.27)	0.08 (2.0)
OHS-R	OPHR	0.047 (1.19)	0 (0)	0.025 (0.64)	0.08 (2.0)
	IPHR	0.061 (1.55)	0.091 (2.31)	0.05 (1.27)	

Notes: OPHR is outside plastic hinge region; IPHR is inside plastic hinge region; NA is not available.

NHS1-R and NHS2-R. A jacket gap of 0.75 in. (19 mm) was specified at the ends of the columns to prevent jacket bearing against the footing or the cap beam under large rotations.

CFRP JACKET DESIGN FOR SUBSTANDARD COLUMNS

The repair of substandard column models was designed with the objective of upgrading shear strength, preventing lap-splice slippage, and upgrading confinement of the columns by using unidirectional CFRP fabrics. The thickness of CFRP for shear strength was calculated using the method described previously. The existing steel hoop contribution to the shear strength was neglected in the repaired substandard column models because the amount of the transverse steel was minimal. Due to reasons discussed previously, the shear strength of the concrete inside the plastic hinge region was neglected, but 50% of the concrete shear strength outside the plastic hinge region was accounted for in the repair design.

The method proposed by Priestley et al. (1996) was used to design the required CFRP jacket thickness to prevent splice failure. They showed that the propensity for splice failure could be predicted by assessment of the concrete tensile capacity across a potential splitting failure surface. After cracking develops on this surface, splice failure can be inhibited with sufficient clamping pressure provided by a CFRP jacket with a radial dilation strain limit of 1500 $\mu\epsilon$ across the fracture surface.

In the absence of *repair* methods, the seismic *retrofit* guidelines of Caltrans (2007) were used to design for confinement provided by the CFRP jacket.

The required and actual thicknesses of the CFRP jackets are listed in Table 2. The jacket for OHS-R consisted of two layers of CFRP along the entire column height and the jacket for OLS-R consisted of two layers of CFRP at the plastic hinge region and one layer of CFRP elsewhere. The results show that inhibiting lap-splice failure governed the jacket design in the plastic hinge regions of both columns. Caltrans (2007) confinement requirements controlled the jacket design outside the plastic hinge regions in OLS-R, and shear strength requirements governed the jacket design outside the plastic hinge regions of OHS-R. According to Table 2, a CFRP thickness of 0.091 in. (2.31 mm) was required to inhibit lap-splice failure in OHS-R. Two layers of CFRP with a thickness of 0.08 in. (2.0 mm) were used in OHS-R instead of a three-layer jacket with a thickness of 0.12 in. (3.0 mm) to prevent an overly conservative jacket design.

Similar to the standard columns, a 0.75 in. (19 mm) gap was specified at the ends of the jackets.

REPAIR PROCEDURE

The entire repair work took 3 to 4 days for each column and consisted of the following steps:

Straightening columns

The residual drift ratio in Bent-2, NHS1, and NHS2 at the end of the test was 10.4%, 3.35%, and 2.0%, respectively. Prior to repair, the bent and the columns were straightened to a near-vertical position (1% or less drift ratio) by adjusting the shake tables. The residual drift ratios in OLS and OHS were relatively small at 0.55% and 0.21%, respectively, and the columns were not straightened. In practice, straightening would vary, depending on the bridge, extent of residual displacement, and the bridge surroundings. Pulling the bridge using heavy-duty construction equipment may be an option.

Removal of loose concrete

The loose concrete was removed by an impact hammer with a chisel head (Fig. 4). The area was cleaned using compressed air to remove dust and the remaining concrete particles after chipping the concrete. No loose concrete was observed in the original substandard columns after the tests. Therefore, this step was not exercised for these columns.

Concrete repair

Two different types of mortar and placement methods were used. In NHS1-R, a low-shrinkage repair mortar with 1-day and 3-day specified compressive strengths of 2.5 and 4 ksi (17.2 and 27.6 MPa), respectively, was used. A thick mortar was made and applied to the spalled area by hand and consolidated by thumb pressure. The compressive strength of the mortar was 4.05 ksi (27.9 MPa) on the test day when the mortar was 3 days old. In Bent-2R, NHSR-2, and OLS-R, a low-shrinkage, fast-setting repair mortar with 3-hour and 1-day specified compressive strengths of 3 and 4 ksi (20.7 and 27.6 MPa), respectively, was used. The specified Young's modulus of this mortar was 3800 ksi (26.2 GPa). Due to the relatively high 1-day compressive strength for the second mortar, it was decided to make a fluid mortar and cast it into a mold instead of patching it in the spalled area (Fig. 4). The mortar was consolidated using a small vibrator. The compressive strength of the mortar used in NHS2-R was 7.87 ksi (54.3 MPa) on the test day at the age of 4 days.



Fig. 4—Rapid repair procedure.

Epoxy injection

To provide integrity and stiffness for the damaged columns, the cracks were injected with epoxy at a pressure of 40 to 50 psi (0.28 to 0.34 MPa). To inject the epoxy, several ports were attached on all the visible cracks and the crack surfaces were sealed with a removable sealer. Epoxy was injected into a given crack through one port and injection was continued until bleeding from another port occurred. The epoxy injection process is shown in Fig. 4.

Surface preparation and CFRP wrapping

After the concrete was repaired and epoxy was injected, the column surface was smoothed slightly by a grinder to remove any surface roughness and any injected material residues from the column surface. A layer of epoxy was applied to prime the column surfaces (Fig. 4). Subsequently, a thickened epoxy was applied directly on the columns to smooth out imperfections. After preparing the surface, the epoxy was applied to CFRP layers using a paint roller and the sheets were wrapped around the columns manually (Fig. 4).

Accelerated curing of jacket

The entire curing of the jacket took approximately 48 hours for each column and consisted of accelerated curing for the first 24 hours, followed by curing under the laboratory ambient condition. Note that specifications call for a minimum of 7 days of curing for CFRP jackets in the ambient condition. During accelerated curing, the temperature was elevated to 110°F (43°C) and the relative humidity was reduced to 15% by covering the area around the models with plastic sheets (Fig. 4), using heat lamps directed away from the columns and electric heaters, and a fan for circulation. This condition was maintained for approximately 24 hours. The plastic sheet was subsequently removed to allow for installation of strain gauges and linear variable differential transformer (LVDT) displacement transducers. The jackets were cured at the ambient temperature in the laboratory for an additional 24 hours.

CFRP MATERIAL PROPERTIES

The design and measured modulus of elasticity and measured rupture strain of the CFRP material are listed in Table 3. CFRP properties recommended by Caltrans (Steckel

Table 3—CFRP material properties

Model	Modulus of elasticity, ksi (GPa)		Measured rupture strain, $\mu\epsilon$
	Design	Measured	
Bent-2R	8000 (55.2)	8215 (56.6)	10,562
NHS1-R	8000 (55.2)	10,306 (71.1)	11,440
NHS2-R	10,000 (69.0)	13,468 (92.9)	8415
OLS-R	12,000 (82.7)	12,310 (84.9)	8699
OHS-R	12,000 (82.7)	14,453 (99.7)	9907

et al. 1999) were used in the jacket design of Bent-2R. For other columns, the measured properties of the CFRP from previous tests—but limited to the specified properties—were used in the jacket design. The measured properties were determined based on coupon tests. The coupons were cured under the same conditions as those of the column jackets. The specified modulus of elasticity and rupture strain of the CFRP after full curing were 11,900 ksi (82.0 GPa) and 10,000 $\mu\epsilon$, respectively. In all columns, the measured modulus of elasticity exceeded the design value, indicating that the accelerated curing was effective. The average measured rupture strain was comparable to the specified value.

EXPERIMENTAL RESULTS FOR REPAIRED COLUMNS

The repaired bent and columns were tested on shake tables under generally the same loading protocols as those used in the original bent and column tests. The main difference was that the loading protocols for the repaired columns included additional runs with increasing amplitudes until failure.

In Bent-2R, no damage was observed during the shake-table runs until the drift ratio of 9.0%. At this drift ratio, the first CFRP rupture occurred in the column under compressive force due to the overturning moment (west column). This rupture was extended during subsequent runs. The second CFRP rupture was observed in the east column during the last run at a 13.1% drift ratio. The ruptured jackets in both columns are shown in Fig. 5. After the shake-table test, the CFRP jacket and some concrete were removed from the plastic hinge regions and no ruptured bar was observed (Fig. 5).

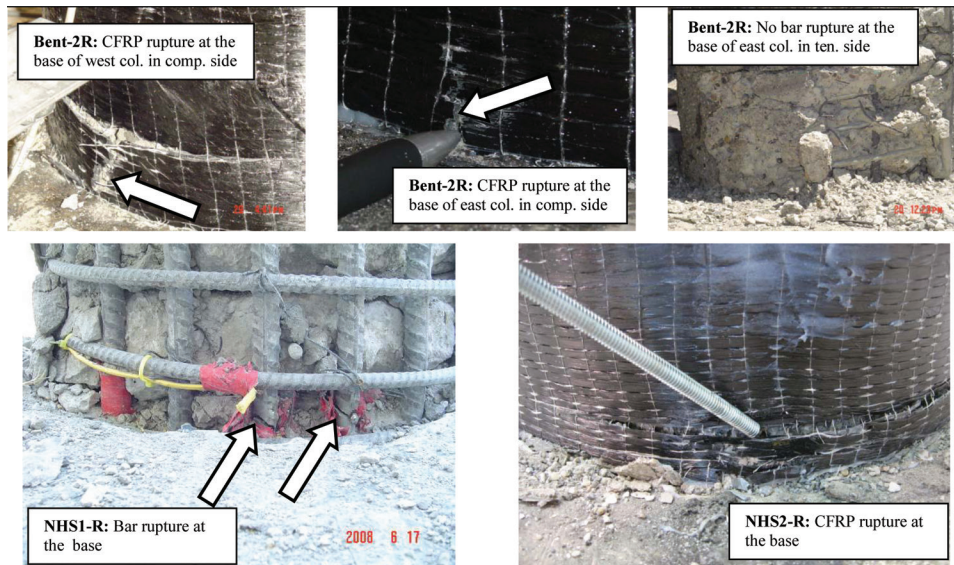


Fig. 5—Repaired columns after shake-table test.

Table 4—Measured responses of repaired columns

Model	Yield drift, %	Ultimate drift, %	Strength, kips (kN)
Bent-2R	1.52	13.11	33.5 (149)
NHS1-R	4.16	13.10	90.3 (402)
NHS2-R	2.56	13.31	85.7 (381)
OLS-R	1.80	5.64	26.6 (118)
OHS-R	1.29	4.57	63.8 (284)

In NHS1-R, no damage was observed during the test. During the last run, a sound of steel rupture was heard. After removal of the jacket and some concrete, two broken longitudinal bars were found at the column base (Fig. 5). Removal of the jacket and concrete at the column top did not reveal any ruptured bars.

In NHS2-R, no damage was observed during the test until a drift ratio of 9.94%. The jacket ruptured over an approximately 0.25 in. (6 mm) area at the column base at this drift ratio. This rupture was extended during the subsequent run, which was the last one (Fig. 5). The maximum measured drift ratio was 13.3% during this run. During the last run, the CFRP rupture was accompanied by a sound of steel rupture. After removal of the jacket and some concrete, two broken longitudinal bars were found at the column base. No bar fractures were noted at the top plastic hinge after removal of the jacket and concrete in NHS2-R.

No damage was observed in OLS-R and OHS-R during the tests. During the last run, the sound of steel rupture was heard. After removal of the jacket and some concrete, a broken longitudinal bar was found in the primary tension side of each column base. Removal of the jacket and concrete at the top of OHS-R did not reveal any ruptured bars.

The CFRP jackets were extensively instrumented with strain gauges in the plastic hinge regions. The jacket ruptured in Bent-2R and NHS2-R. The maximum measured strain in the NHS2-R jacket was 9410 $\mu\epsilon$ prior to the failure. The measured jacket strain capacity in the coupon test (Table 3) was smaller due to strain concentrations at the grips of the test machine. In NHS1-R, the maximum measured jacket

strain was 4932 $\mu\epsilon$. The peak strain was developed at the top plastic hinge on the compressive side of the column, where the role of the CFRP jacket was to provide confinement. The peak strain was comparable with the design strain of 4000 $\mu\epsilon$. In OLS-R, a maximum jacket strain of 3597 $\mu\epsilon$ was developed at the column base on the primary compression side. This strain was smaller than the design strain of 4000 $\mu\epsilon$. In OLS-R, the maximum measured strain due to the clamping force in the lap splice was 1191 $\mu\epsilon$, which was smaller than the design strain of 1500 $\mu\epsilon$. In OHS-R, the maximum recorded CFRP strain was 3811 $\mu\epsilon$ at the column base. The peak strain was on the side of the column where strains due to column shear were developed and was smaller than the design strain of 4000 $\mu\epsilon$.

In the substandard repaired columns, the longitudinal bar strains were measured along the lap splice. Using the approach discussed previously, it was concluded that no slippage occurred in the lap splices based on the measured strains. This indicates that the jacket provided sufficient confinement to prevent splice failure, even under large deformations.

The yield drift ratio, ultimate drift ratio, and lateral load strength of the repaired columns were determined using idealized elasto-plastic envelope curves and are listed in Table 4. The data show that the confinement and lateral load strength of the substandard columns were upgraded effectively because the repaired columns underwent a reasonable plastic deformation before failure.

EVALUATION OF REPAIR PERFORMANCE

The force-displacement response of the original and repaired column models were used to evaluate the repair performance. The measured force-displacement envelopes of all column models are shown in Fig. 3(d) to (h). It should be noted that the end points in the original models do not indicate failure because these columns were not tested to failure. The ultimate points were estimated using a method described in the following sections (displacement capacity index) and marked on the graphs. The envelopes indicate that the strength and displacement capacity of the columns were fully restored and the stiffness of the models was not restored by the repair. The lower stiffness of the repaired

columns is attributed to the residual plastic strains in longitudinal bars and core concrete degradation.

To quantify the comparison between the original and repaired models, three nondimensionalized response indexes were developed in terms of strength, stiffness, and displacement capacity. The response indexes reveal whether the residual strength, stiffness, and displacement capacity in the damaged column models were restored by the repair. Generally, the residual strength, stiffness, and displacement capacity are smaller than those of the original column due to damage.

Strength index

The column strength was defined as the plastic lateral load capacity of the column (F_p) that was determined using the idealized elasto-plastic force-displacement curves. The ratio between the measured strength of the repaired column and the original column was defined as the strength index. This index is shown as I_s and is calculated as follows

$$I_s = \frac{F'_p}{F_p} \quad (1)$$

where F'_p and F_p are the lateral strengths of the repaired and original columns, respectively. A strength index equal to or greater than 1 indicates that the column strength was fully restored through the repair. The strength index is plotted in Fig. 6 for all columns. It can be seen that the strength index is greater than 1 for all repaired columns, thus indicating that the repairs were successful. Due to insufficient transverse steel, the shear strength of OHS was significantly lower than its plastic flexural capacity. After repair, the shear strength was increased and OHS-R reached the plastic lateral load capacity. Consequently, a considerably high-strength index is observed for this column.

Service stiffness index

The serviceability of a structure is addressed based on the elastic stiffness of the structure. The ratio between the elastic stiffness of the repaired column and the original column was defined as the service stiffness index. This index is shown as I_{ss} and is calculated as follows

$$I_{ss} = \frac{K'}{K} \quad (2)$$

where K' and K are the elastic stiffnesses of the repaired and original columns, respectively. The elastic stiffness of the columns was defined as the initial slope in the idealized elasto-plastic force-displacement relationship. Indexes equal to or greater than 1 indicate that the column service stiffness was fully restored by the repair. The index was calculated for all column models and is plotted in Fig. 6. The plots show that all of the indexes are smaller than 1, meaning that the stiffness of the repaired columns was smaller than that of the original columns due to the reasons discussed previously. In addition, the fact that the epoxy injection of the cracks could not fill the relatively thin cracks in the original column led to stiffness degradation of concrete.

The service stiffness index in the substandard columns was higher than that of the standard columns because the damage level in the original substandard columns was lower than that of the standard columns. Therefore, the stiffness

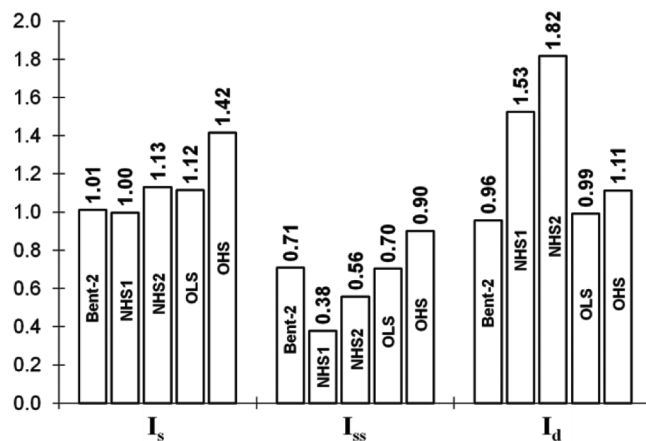


Fig. 6—Nondimensionalized response indexes.

deterioration in the original substandard columns was less significant—particularly in OHS, where the maximum damage state in the original column was DS-2.

Among the standard columns, NHS1 had the smallest service stiffness index because the repair mortar was not of high quality and its consolidation method was less effective in NHS1 than those of other columns. As discussed previously, the water-cement ratio (w/c) in the repair mortar of NHS1 was reduced due to the relatively low strength of the mortar, and the mortar was placed by hand because of its low workability. Furthermore, the mortar was consolidated by thumb pressure. In Bent-2 and NHS2, due to the high quality of the repair mortar, a fluid mortar was prepared and cast into the mold around the damaged zone. This was followed by consolidation using a small vibrator, which was more effective.

Displacement capacity index

The ratio between the measured displacement capacity of the repaired and original columns was defined as the displacement capacity index. This index is shown as I_d and is calculated as follows

$$I_d = \frac{\Delta'_c}{\Delta_c} \quad (3)$$

where Δ'_c and Δ_c are the displacement capacities of the repaired and original models, respectively. The original columns were tested on the shake table up to the highest target repairable damage state, which does not constitute failure. This damage state is referred to as “imminent failure.” Therefore, the ultimate displacement capacity for the original columns needed to be estimated before I_d could be found. In a previous study (Vosooghi and Saiidi 2010b), it was shown that at a damage state of “imminent failure,” standard low-shear and high-shear columns reach 0.74 and 0.85 of their plastic displacement capacity, respectively. Consequently, the ultimate displacement of Bent-2 was estimated by increasing the maximum measured plastic displacement by 35% and that of NHS1 and NHS2 was estimated by increasing the maximum measured displacement by 18%. Plastic displacement was calculated based on idealized elasto-plastic curves.

Indexes equal to or greater than 1 indicate that the column displacement capacity was fully restored by the repair. As mentioned previously, the substandard columns were

repaired and retrofitted simultaneously. The objective of the retrofit was to satisfy the current seismic design codes. Therefore, instead of using the displacement capacity of the original columns (Δ_c), the displacement corresponding to a target displacement ductility of 5 was used to calculate the displacement capacity index for the substandard columns.

The displacement capacity indexes for all column models are plotted in Fig. 6. It can be seen that the index was close to 1 in Bent-2 and OLS and was greater than 1 in the remaining column models. This indicates that the displacement capacity of the column models was fully restored by the repair.

Figure 6 shows that the indexes of NHS2 were generally higher than those of NHS1, even though the number of CFRP layers in NHS2 was lower. The results demonstrate that the repair procedure in terms of quality and the application method of the repair mortar has a significant effect on the performance of the repaired column. It is recommended that only high-early-strength, low-shrinkage grout be used in repair. The improved performance of NHS2-R clearly suggests that the relatively high number of CFRP layers in NHS1-R was unnecessary and counting on 50% of the spiral shear-resisting force in NHS2-R was a reasonable assumption.

Generally, even though the repair process was done rapidly and was treated as “emergency” repair with the implication that it was a temporary measure, it can be treated as a permanent repair as long as the stiffness of the repaired columns is sufficient under nonseismic loads.

CONCLUSIONS

The following conclusions were drawn based on the results presented in this paper:

- The proposed accelerated curing method for the CFRP jacket was effective and reduced the required repair time significantly.
- The proposed rapid repair procedure using CFRP for earthquake-damaged standard RC bridge columns to the highest damage state with no bar rupture was effective in restoring the shear strength and displacement ductility capacity.
- The repair procedure in terms of quality and the application method of the repair mortar had a significant effect on the performance of the repaired columns. High-early-strength, low-shrinkage grout should be used in repair.
- Counting on 50% of the shear strength of transverse steel in the high-shear columns was a reasonable assumption in CFRP jacket design and led to a significant reduction in the required jacket thickness.
- The proposed rapid repair procedure using CFRP for earthquake-damaged substandard RC bridge columns to the highest damage state with no shear and/or splice failure was effective in upgrading the shear strength and displacement ductility capacity and inhibiting splice failure.
- Due to stiffness degradation of the steel and the concrete during the original model tests and uninjected microcracks, the stiffness of the columns could not be fully restored by the repair.
- Even though the repair process was done rapidly and was treated as “emergency” repair with the implication that it was a temporary measure, it can be treated as a permanent repair as long as the stiffness of the repaired columns is sufficient under nonseismic loads.

ACKNOWLEDGMENTS

This research project was funded by the California Department of Transportation (Caltrans) through Grant No. 59A0543. The conclusions and

recommendations are those of the authors and do not necessarily present the views of the sponsor. The authors wish to thank S. El-Azazy for his helpful comments and support and J. Gutierrez for his instrumental role in the application of repair work and his close interaction. The authors also wish to thank S. Arnold of the Fyfe Company for arranging for material donation.

REFERENCES

- ACI Committee 318, 2008, “Building Code Requirements for Structural Concrete (ACI 318-08) and Commentary,” American Concrete Institute, Farmington Hills, MI, 473 pp.
- Belarbi, A.; Silva, P.; and Bae, S., 2008, “Retrofit of RC Bridge Columns under Combined Axial, Shear, Flexure, and Torsion Using CFRP Composites,” *Bridge Science and Applications with Engineering Towards Innovative Solutions for Construction*, Challenges for Civil Construction, Porto, Portugal, Apr. 16-18, 10 pp.
- Caltrans, 2003, “Bridge Design Specifications,” California Department of Transportation, Sacramento, CA.
- Caltrans, 2006, “Seismic Design Criteria (SDC),” version 1.4, California Department of Transportation, Sacramento, CA.
- Caltrans, 2007, “Memo to Designers 20-4, Attachment B,” California Department of Transportation, Sacramento, CA, 3 pp.
- Choi, H.; Saiidi, M.; and Somerville, P., 2007, “Effects of Near-Fault Ground Motion and Fault-Rupture on the Seismic Response of Reinforced Concrete Bridges,” *Report No. CCEER-07-06*, Center for Civil Engineering Earthquake Research, University of Nevada, Reno, NV, 559 pp.
- Haroun, M. A., and Elsanadedy, H., 2005, “Fiber-Reinforced Plastic Jackets for Ductility Enhancement of Reinforced Concrete Bridge Columns with Poor Lap-Splice Detailing,” *Journal of Bridge Engineering*, ASCE, V. 10, No. 6, pp. 749-757.
- Johnson, N.; Ranf, T.; Saiidi, M.; Sanders, D.; and Eberhard, M., 2008, “Seismic Testing of a Two-Span Reinforced Concrete Bridge,” *Journal of Bridge Engineering*, ASCE, V. 13, No. 2, pp. 173-182.
- Laplace, P.; Sanders, D.; and Saiidi, M., 1999, “Shake Table Testing of Flexure Dominated Reinforced Concrete Bridge Columns,” *Report No. CCEER-99-13*, Center for Civil Engineering Earthquake Research, University of Nevada, Reno, NV, 163 pp.
- Laplace, P. N.; Sanders, D.; Saiidi, M.; Douglas, B.; and El-Azazy, S., 2005, “Retrofitted Concrete Bridge Columns Under Shaketable Excitation,” *ACI Structural Journal*, V. 102, No. 4, July-Aug., pp. 622-628.
- Lehman, D. E.; Gookin, S.; Nacamuli, A.; and Moehle, J., 2001, “Repair of Earthquake-Damaged Bridge Columns,” *ACI Structural Journal*, V. 98, No. 2, Mar.-Apr., pp. 233-242.
- Li, Y. F., and Sung, Y., 2003, “Seismic Repair and Rehabilitation of a Shear-Failure Damaged Circular Bridge Column Using Carbon Fiber Reinforced Plastic Jacketing,” *Canadian Journal of Civil Engineering*, V. 30, pp. 819-829.
- Priestley, M. J. N., and Seible, F., 1993, “Repair of Shear Column Using Fiberglass/Epoxy Jacket and Epoxy Injection,” *Report No. 93-04*, Job No. 90-08, Seqad Consulting Engineers, Solana Beach, CA, July.
- Priestley, M. J. N.; Seible, F.; and Calvi, G. M., 1996, *Seismic Design and Retrofit of Bridges*, John Wiley & Sons, Inc., New York, 704 pp.
- Saadatmanesh, H.; Ehsani, M.; and Jin, L., 1996, “Seismic Strengthening of Circular Bridge Pier Models with Fiber Composites,” *ACI Structural Journal*, V. 93, No. 6, Nov.-Dec., pp. 639-647.
- Saadatmanesh, H.; Ehsani, M.; and Jin, L., 1997, “Repair of Earthquake-Damaged RC Columns with FRP Wraps,” *ACI Structural Journal*, V. 94, No. 2, Mar.-Apr., pp. 206-215.
- Saiidi, M., and Cheng, Z., 2004, “Effectiveness of Composites in Earthquake Damage Repair of RC Flared Columns,” *Journal of Composites for Construction*, ASCE, V. 8, No. 4, pp. 306-314.
- Seible, F.; Priestley, M. J. N.; Hegemier, G.; and Innamarate, D., 1997, “Seismic Retrofit of RC Columns with Continuous Carbon Fiber Jackets,” *Journal of Composites for Construction*, ASCE, V. 1, No. 2, pp. 52-62.
- Steckel, G. L.; Hawkins, G. F.; and Bauer, J. L., 1999, “Qualifications for Seismic Retrofitting of Bridge Columns Using Composites,” *Aerospace Report No. ATR-99(7524)-2*, Aerospace Corporation, El Segundo, CA, Prepared for California Department of Transportation, Jan.
- Vosooghi, A., and Saiidi, M., 2010a, “Post-Earthquake Evaluation and Emergency Repair of Damaged RC Bridge Columns Using CFRP Materials,” *Report No. CCEER-10-05*, Center for Civil Engineering Earthquake Research, University of Nevada, Reno, NV, 636 pp.
- Vosooghi, A., and Saiidi, M., 2010b, “Seismic Damage States and Response Parameters for Bridge Columns,” *Structural Concrete in Performance-Based Seismic Design of Bridges*, SP-271, P. F. Silva and R. Valluvan, eds., American Concrete Institute, Farmington Hills, MI, pp. 27-44.